BOUNDARY CONTROL DESIGN FOR TOWED CABLES VIA BACKSTEPPING

Yilmaz Türkyilmaz and Olav Egeland

Dept. of Eng. Cybernetics, Norwegian Univ. of Science and Technology, 7491 Trondheim, Norway.
fax: (+47) 73 59 43 99
e-mail: {yilmaz, oe}@itk.ntnu.no

Keywords: Marine Systems, Towed Cables, Boundary Control, Backstepping, Lyapunov Stability

Abstract

A boundary control design for towed cables via backstepping is presented. A towed cable model is discretized by the finite element method into n nodes. The boundary control law is designed using the states at the outer nodes as inputs to stabilize the states at the inner nodes, thus moving backwards to construct a controller that can stabilize all system states asymptotically. The boundary controller improves the transient dynamics, suppresses the vibrations and enables smooth tracking for the towed cable system. Simulation and numerical results are presented to validate the proposed boundary control law.

1 Introduction

Towing of cables is a method used extensively in marine operations. A typical cable-towing configuration consists of a negatively buoyant cable attached to a towing vessel and, at the other end, to a submersible, which may contain sensor equipment and an actuator for depth control. Accurate control of the cable motion is of great importance in seismic operations. A towing arrangement with is illustrated in Figure (1).

The dynamics of the cables/strings have been studied by many authors: [4], [8], [5], [13], [6], [9] and the references therein. Boundary control aspects of the cable/string systems have been investigated by several authors. Among others, [7] designed a boundary feedback controller for a system described by the wave equation where exponential stability of the closed loop is obtained for strictly proper transfer functions. [2] developed exponentially stabilizing controllers for the transverse vibration of a string-mass system modeled by one-dimensional wave equation. [12] and [3] devised exponentially stabilizing controllers for a one-dimensional nonlinear string equation, allowing varying tension in the string. [10] devised a robust and adaptive controller to damp out the transverse oscillations of a stretched string, allowing nonlinear dynamics and their uncertainties in the model. The works mentioned above use a combination of the states at the boundary, namely the boundary position, slope, slope-rate and velocity, to design the stabilizing boundary control laws.

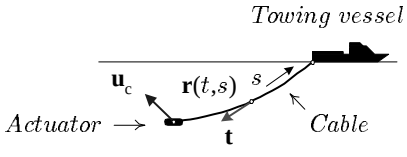

Figure 1: A towing configuration.

In this paper, we extend the previous works taking into account additional states that might be available through observers or direct measurements, at specified positions along the cable/string system and propose a solution that uses such information in the control of the motion of a towed cable. The boundary control law is designed via the backstepping method, considering a towed cable model that is discretized by the finite element method into n nodes. The boundary control law is then constructed using the states at the outer nodes as inputs to stabilize the states at the inner nodes, thus moving backwards along the cable to construct a controller that can stabilize all the system states asymptotically. The simulation and numerical results are presented to validate the proposed boundary control law.

2 Cable Dynamics

2.1 Equation of Motion

Consider a cable of length $L \in \mathbb{R}$ with negligible bending and torsional stiffness. The unstretched distance along the average line of the cable is denoted by $s \in [0, L]$ and the stretched distance by s_e. The axial strain of the cable is then $e = (\partial s_e - \partial s) / \partial s$. Let $\mathbf{r}(t, s) : [t_0, \infty) \times [0, L] \to \mathbb{R}^3$ be the position vector of an arbitrary point on the average line of the cable where t is the time variable. The unit vector $\mathbf{t}(t, s) \in \mathbb{R}^3$ tangent to the cable is defined as $\mathbf{t}(t, s) = \partial \mathbf{r} / \partial s_e$ which can be rewritten as

$$\mathbf{t}(t, s) = \frac{\partial \mathbf{r}}{\partial s} \frac{\partial s}{\partial s_e} = \frac{1}{1 + e} \frac{\partial \mathbf{r}}{\partial s} \tag{1}$$

The equation of motion of a cable is [13] given by

$$m \frac{\partial^2 \mathbf{r}(t, s)}{\partial t^2} = \frac{\partial}{\partial s} \left[T(t, s) \mathbf{t}(t, s) \right] + \mathbf{q}(t, s) \left[1 + e \right] \tag{2}$$

where is $m \in \mathbb{R}$ mass per unit length of unstretched cable, $T \in \mathbb{R}$ is the tension and $\mathbf{q} \in \mathbb{R}^3$ is the sum of external forces per unit length of unstretched cable acting on the cable. For a submerged cable, it is assumed that the external forces consist of the buoyancy force $\mathbf{q}_b$ and the hydrodynamic drag force $\mathbf{q}_d$.

These forces are given by

$$\begin{aligned}\mathbf{q}_b &= m\left[\left(\rho_w-\rho_c\right)/\rho_c\right]\mathbf{g}\\ \mathbf{q}_d &= -\frac{1}{2}C_{dt}\rho_w d\left|\mathbf{v}\cdot\mathbf{t}\right|\left(\mathbf{v}\cdot\mathbf{t}\right)\mathbf{t}\\ &\quad -\frac{1}{2}C_{dt}\rho_w d\left|\mathbf{v}-\left(\mathbf{v}\cdot\mathbf{t}\right)\mathbf{t}\right|\left(\mathbf{v}-\left(\mathbf{v}\cdot\mathbf{t}\right)\mathbf{t}\right)\end{aligned}$$

where $\mathbf{g}\in\mathbb{R}^3$ is the gravitational acceleration, ρ_c the density of the cable, ρ_w is the density of the ambient water, C_{dt} and C_{dn} are the tangential and normal drag coefficients of the cable, respectively, d is the cable diameter. The cable velocity $\mathbf{v}\in\mathbb{R}^3$ is given by $\mathbf{v}=\dot{\mathbf{r}}-\boldsymbol{v}$ where $\boldsymbol{v}$ is the relative velocity of the fluid surrounding the cable due to vessel's marching speed and sea current, and it is assumed to be constant. Applying Hooke's law, $T=EAe$ where E is the Young's modulus and A is the cross-sectional area of the unstretched cable, and using (1) in (2) gives

$$m\frac{\partial^2\mathbf{r}}{\partial t^2}=\frac{\partial}{\partial s}\left[EA\frac{e}{1+e}\frac{\partial\mathbf{r}}{\partial s}\right]+\mathbf{q}\left[1+e\right] \tag{3}$$

with the boundary conditions

$$\mathbf{r}\left(t,0\right)=\mathbf{b}_1\left(t\right),\quad \mathbf{r}\left(t,L\right)=\mathbf{b}_2\left(t\right)$$

for all $t\geq t_0$, and the initial conditions

$$\mathbf{r}\left(t_0,s\right)=\mathbf{b}_3\left(s\right),\quad \mathbf{v}\left(t_0,s\right)=\mathbf{b}_4\left(s\right)$$

where $\mathbf{b}_1\left(t\right)$, $\mathbf{b}_2\left(t\right)$ are functions of time t, and $\mathbf{b}_3\left(s\right)$, $\mathbf{b}_4\left(s\right)$ are the initial cable configuration and cable velocity respectively.

2.2 FEM model for the Cable Dynamics

A finite element model, based on the Galerkin approximation, is derived [1] from the nonlinear PDE describing the cable dynamics in (3). The cable is divided into n elements, where the length of each element is $l=L/n$, and the nodal points are enumerated from 0 to n where $s=0$ is the actuator node, and $s=L$ is tow-point. The simplified finite element model for the cable is given by

$$\begin{aligned}&ml\ddot{\mathbf{r}}_k+EA\left[\left(e_k/\epsilon_k\right)\mathbf{h}_k-\left(e_{k+1}/\epsilon_{k+1}\right)\mathbf{h}_{k+1}\right]+\\ &\qquad ml\left[\left(\rho_w-\rho_c\right)/\rho_c\right]\mathbf{g}+\\ &\qquad c_1\left(\left|\mathbf{v}_k\cdot\mathbf{h}_{k+1}\right|\boldsymbol{\gamma}_{k+1}\right)\mathbf{v}_k+\\ &c_2\left[\epsilon_{k+1}\left|\left(\mathbf{I}_{3\times3}-\boldsymbol{\gamma}_{k+1}\right)\mathbf{v}_k\right|\left(\mathbf{I}_{3\times3}-\boldsymbol{\gamma}_{k+1}\right)\right]\mathbf{v}_k \;=\; \boldsymbol{\tau}_k\end{aligned} \tag{4}$$

for $k=1,...,n-1$, where $\mathbf{I}_{3\times3}\in\mathbb{R}^{3\times3}$ is the identity matrix, $\boldsymbol{\tau}_k\in\mathbb{R}^3$ is the control input at node k, and

$$\begin{aligned}\boldsymbol{\gamma}_k &= \mathbf{h}_k\mathbf{h}_k^T/\epsilon_k^2 && (5)\\ \mathbf{h}_k &= \mathbf{r}_k-\mathbf{r}_{k-1} && (6)\\ e_k &= \left|\mathbf{h}_k\right|/l-1 && (7)\\ \epsilon_k &= \left|\mathbf{h}_k\right| && (8)\\ \mathbf{v}_k &= \dot{\mathbf{r}}_k-\boldsymbol{v} && (9)\\ c_1 &= 0.5C_{dt}d\rho_w\\ c_2 &= 0.5C_{dn}d\rho_w\end{aligned}$$

Note that by excluding bending stiffness from cable model in (2), we introduce a *zero tension singularity* which occurs in the absence of positive tension. Thus, cable may display a discontinuous form such that (2) is ill-posed. Requiring positive tension implies $\left|\mathbf{h}_k\right|>l$ and $0<e_k/\epsilon_k<1/l$ such that system equations in (4) can be simplified further by approximating $0<e_k/\epsilon_k\approx\mu<1/l$ where $\mu>0$. This approximation eliminates the dependence of the terms e_k/ϵ_k on the system states, which in practice means one assumes that the elongation in each segment is uniform. In (4), the drag forces along the downstream neighboring elements are ignored to simplify the implementation. In addition, the mass of two neighboring elements are lumped at the corresponding node. This gives a *nonconsistent mass-matrix* [11]. A set of nonlinear ODEs for the cable and the actuator can now be put into form

$$\begin{aligned}ml\ddot{\mathbf{r}}_{n-1} &= -\mathbf{D}_{n-1}\dot{\mathbf{r}}_{n-1}+\mathbf{q}_{n-1}\\ &\quad -EA\left[\mu\mathbf{h}_{n-1}-\mu\mathbf{h}_n\right]-\mathbf{g}_{n-1} && (10)\\ \vdots &= \vdots\\ ml\ddot{\mathbf{r}}_1 &= -\mathbf{D}_1\dot{\mathbf{r}}_1+\mathbf{q}_1 && (11)\\ &\quad -EA\left[\mu\mathbf{h}_1-\mu\mathbf{h}_2\right]-\mathbf{g}_1\\ \mathbf{M}\ddot{\mathbf{r}}_0 &= -\mathbf{D}_0\dot{\mathbf{r}}_0+\mathbf{q}_0+EA\mu\mathbf{h}_1-\mathbf{g}_0+\mathbf{u}_c && (12)\end{aligned}$$

where for $k=1,...,n-1$

$$\begin{aligned}\mathbf{g}_k &= ml\left[\left(\rho_w-\rho_c\right)/\rho_c\right]\mathbf{g}\\ \mathbf{D}_k &= c_1\left(\left|\mathbf{v}_k\cdot\mathbf{h}_{k+1}\right|\boldsymbol{\gamma}_{k+1}\right)\\ &\quad +c_2\left[\epsilon_{k+1}\left|\left(\mathbf{I}_{3\times3}-\boldsymbol{\gamma}_{k+1}\right)\mathbf{v}_k\right|\left(\mathbf{I}_{3\times3}-\boldsymbol{\gamma}_{k+1}\right)\right]\\ \mathbf{q}_k &= \mathbf{D}_k\boldsymbol{v}\end{aligned}$$

for the cable and

$$\begin{aligned}\mathbf{g}_0 &= \left(m_a-\rho_w V_a\right)\mathbf{g}\\ \mathbf{D}_0 &= \mathrm{diag}\{d_1\left|\mathbf{v}_0\right|,d_2\left|\mathbf{v}_0\right|,d_3\left|\mathbf{v}_0\right|\}\\ \mathbf{q}_0 &= \mathbf{D}_0\boldsymbol{v}\end{aligned}$$

where $\mathbf{M}=m_a\mathbf{I}_{3\times3}$ is the mass matrix, m_a is the mass and V_a is the volume of the actuator. $\mathbf{g}_0\in\mathbb{R}^3$ is the buoyancy force vector and $\mathbf{D}_0\in\mathbb{R}^{3\times3}$ is the damping matrix where $d_1,\ldots,d_3$ are the damping coefficients and $\mathbf{v}_0=\dot{\mathbf{r}}_0-\boldsymbol{v}$ is the velocity vector. $\mathbf{q}_0\in\mathbb{R}^3$ is the hydrodynamic damping vector due to the relative velocity $\boldsymbol{v}$, for the actuator. The dynamics of the towing vessel is not included into system equations other than being considered as a point moving with a certain commanded speed. Finally, $\mathbf{u}_c\in\mathbb{R}^3$ is the boundary control input generated by the actuator which we wish to design via the backstepping method.

3 Boundary Control Design via Backstepping

The basic idea in the design of boundary control input can be summarized as follows; the states at the outer nodes are used as inputs to stabilize the states at the inner nodes, thus moving towards the actuator to design a boundary control input that can stabilize all the system states. This is illustrated in Figure 2. To apply the backstepping method in the boundary control design, the simplified system equations in (10)–(12) will be rearranged

into a form with the following structure

$$\begin{aligned}
\dot{\mathbf{e}}_1 &= \mathbf{f}_1(\mathbf{e}_1) + \mathbf{G}_1(\mathbf{e}_1)\mathbf{e}_2 && (13)\\
\dot{\mathbf{e}}_2 &= \mathbf{f}_2(\mathbf{e}_1,\mathbf{e}_2) + \mathbf{G}_2(\mathbf{e}_1,\mathbf{e}_2)\mathbf{e}_3 && (14)\\
\vdots &= \vdots\\
\dot{\mathbf{e}}_{2n} &= \mathbf{f}_{2n}(\mathbf{e}_1,\ldots,\mathbf{e}_{2n}) + \mathbf{G}_{2n}(\mathbf{e}_1,\ldots,\mathbf{e}_{2n})\mathbf{u}_c && (15)
\end{aligned}$$

where $\mathbf{e}_1,...,\mathbf{e}_{2n}$ are the system states and $\mathbf{u}_c$ is the boundary control input. To do that, we start by setting

$$\begin{aligned}
\mathbf{x}_1 &= \mathbf{r}_{n-1} \quad \Rightarrow \quad \dot{\mathbf{x}}_1 = \dot{\mathbf{r}}_{n-1} = \mathbf{x}_2\\
\mathbf{x}_2 &= \dot{\mathbf{r}}_{n-1} \quad \Rightarrow \quad \dot{\mathbf{x}}_2 = \ddot{\mathbf{r}}_{n-1}\\
\vdots &= \vdots\\
\mathbf{x}_{2n-1} &= \mathbf{r}_0 \quad \Rightarrow \quad \dot{\mathbf{x}}_{2n-1} = \dot{\mathbf{r}}_0 = \mathbf{x}_{2n}\\
\mathbf{x}_{2n} &= \dot{\mathbf{r}}_0 \quad \Rightarrow \quad \dot{\mathbf{x}}_{2n} = \ddot{\mathbf{r}}_0
\end{aligned}$$

where $\mathbf{x}_{2n-1}$ and $\mathbf{x}_{2n}$ are the states at the actuator node. Using those and (5)–(9), we can write (10)–(12) as a set of first-order nonlinear ODEs in the form (for simplicity, here it is only shown for $n = 2$)

$$\begin{aligned}
\dot{\mathbf{x}}_1 &= \mathbf{x}_2 && (16)\\
\dot{\mathbf{x}}_2 &= -\mathbf{c}_3\mathbf{x}_2 - \mathbf{c}_5 - \mu c_4(-\mathbf{r}_2 + 2\mathbf{x}_1 - \mathbf{x}_3) && (17)\\
\dot{\mathbf{x}}_3 &= \mathbf{x}_4 && (18)\\
\dot{\mathbf{x}}_4 &= -\mathbf{c}_6\mathbf{x}_4 - \mathbf{c}_8 + \mu\mathbf{c}_7(-\mathbf{x}_3 + \mathbf{x}_1) + \mathbf{c}_9\mathbf{u}_c && (19)
\end{aligned}$$

where $\mathbf{r}_2$ is the position vector of the tow-point and

$$\begin{aligned}
\mathbf{c}_3 &= (ml)^{-1}\mathbf{D}_1\\
c_4 &= (ml)^{-1}EA\\
\mathbf{c}_5 &= (ml)^{-1}(\mathbf{g}_1 - \mathbf{q}_1)\\
\mathbf{c}_6 &= \mathbf{M}^{-1}\mathbf{D}_0\\
\mathbf{c}_7 &= \mathbf{M}^{-1}EA\\
\mathbf{c}_8 &= \mathbf{M}^{-1}(\mathbf{g}_0 - \mathbf{q}_0)\\
\mathbf{c}_9 &= \mathbf{M}^{-1}
\end{aligned}$$

To obtain the system equations in the form given in (13)–(15), we introduce the error terms, $\mathbf{e}_1...\mathbf{e}_4$

$$\mathbf{e}_i = \mathbf{x}_i - \mathbf{x}_{id} \qquad (20)$$

for $i = 1,...,4$. The equilibrium values, $\mathbf{x}_{1d}...\mathbf{x}_{4d}$ are assumed to be constant. Inserting (20) into (16)–(19) gives the error dynamics

$$\begin{aligned}
\dot{\mathbf{e}}_1 &= \mathbf{f}_1(\mathbf{e}_1) + \mathbf{G}_1(\mathbf{e}_1)\mathbf{e}_2 && (21)\\
\dot{\mathbf{e}}_2 &= \mathbf{f}_2(\mathbf{e}_1,\mathbf{e}_2) + \mathbf{G}_2(\mathbf{e}_1,\mathbf{e}_2)\mathbf{e}_3 && (22)\\
\dot{\mathbf{e}}_3 &= \mathbf{f}_3(\mathbf{e}_1,\ldots,\mathbf{e}_3) + \mathbf{G}_3(\mathbf{e}_1,\ldots,\mathbf{e}_3)\mathbf{e}_4 && (23)\\
\dot{\mathbf{e}}_4 &= \mathbf{f}_4(\mathbf{e}_1,\ldots,\mathbf{e}_4) + \mathbf{G}_4(\mathbf{e}_1,\ldots,\mathbf{e}_4)\mathbf{u}_c && (24)
\end{aligned}$$

where

$$\begin{aligned}
\mathbf{f}_1 &= \mathbf{x}_{2d}\\
\mathbf{f}_2 &= -\mathbf{c}_3(\mathbf{e}_2 + \mathbf{x}_{2d}) - \mathbf{c}_5\\
&\quad +\mu c_4(\mathbf{r}_2 - 2\mathbf{e}_1 - 2\mathbf{x}_{1d} + \mathbf{x}_{3d})\\
\mathbf{f}_3 &= \mathbf{x}_{4d}\\
\mathbf{f}_4 &= -\mathbf{c}_6(\mathbf{e}_4 + \mathbf{x}_{4d}) - \mathbf{c}_8\\
&\quad +\mu\mathbf{c}_7(\mathbf{e}_1 - \mathbf{e}_3 + \mathbf{x}_{1d} - \mathbf{x}_{3d})\\
\mathbf{G}_1 &= \mathbf{I}_{3x3}, \quad \mathbf{G}_2 = \mu c_4, \quad \mathbf{G}_3 = \mathbf{I}_{3x3}, \quad \mathbf{G}_4 = \mathbf{c}_9
\end{aligned}$$

3.1 Backstepping

The design of boundary control input $\mathbf{u}_c$ through the states $\mathbf{e}_3$ and $\mathbf{e}_4$ for (21)–(24) is shown below in detail.

3.1.1 Design of e_3 as Control Input

First, consider the system in (21)–(22) with the following change of variables

$$\begin{aligned}
\boldsymbol{\eta} &= \mathbf{e}_1\\
\boldsymbol{\xi} &= \mathbf{e}_2\\
\mathbf{f}(\boldsymbol{\eta}) &= \mathbf{f}_1(\mathbf{e}_1)\\
\mathbf{G}(\boldsymbol{\eta}) &= \mathbf{G}_1(\mathbf{e}_1)\\
\mathbf{f}_a(\boldsymbol{\eta},\boldsymbol{\xi}) &= \mathbf{f}_2(\mathbf{e}_1,\mathbf{e}_2)\\
\mathbf{G}_a(\boldsymbol{\eta},\boldsymbol{\xi}) &= \mathbf{G}_2(\mathbf{e}_1,\mathbf{e}_2)\\
\mathbf{u} &= \mathbf{e}_3
\end{aligned}$$

this gives

$$\begin{aligned}
\dot{\boldsymbol{\eta}} &= \mathbf{f}(\boldsymbol{\eta}) + \mathbf{G}(\boldsymbol{\eta})\boldsymbol{\xi} && (25)\\
\dot{\boldsymbol{\xi}} &= \mathbf{f}_a(\boldsymbol{\eta},\boldsymbol{\xi}) + \mathbf{G}_a(\boldsymbol{\eta},\boldsymbol{\xi})\mathbf{u} && (26)
\end{aligned}$$

This approach will be exploited repeatedly in the latter derivations to design the boundary control input systematically. Assume that $\mathbf{G}_a(\boldsymbol{\eta},\boldsymbol{\xi}) \neq \mathbf{0}$. Substituting the input transformation

$$\mathbf{u}_a = \mathbf{f}_a(\boldsymbol{\eta},\boldsymbol{\xi}) + \mathbf{G}_a(\boldsymbol{\eta},\boldsymbol{\xi})\mathbf{u} \qquad (27)$$

in (26) gives

$$\begin{aligned}
\dot{\boldsymbol{\eta}} &= \mathbf{f}(\eta) + \mathbf{G}(\eta)\boldsymbol{\xi} && (28)\\
\dot{\boldsymbol{\xi}} &= \mathbf{u}_a && (29)
\end{aligned}$$

Suppose that we can find a smooth state feedback control $\boldsymbol{\xi} = \phi_1(\boldsymbol{\eta})$ such that the origin of $\dot{\boldsymbol{\eta}} = \mathbf{f} + \mathbf{G}\phi_1$ is asymptotically stable. Suppose further that we know a Lyapunov function $V_1(\eta)$ which satisfies the inequality

$$\frac{\partial V_1(\eta)}{\partial \eta}[\mathbf{f} + \mathbf{G}\phi_1] \leq -W_1(\eta) \qquad (30)$$

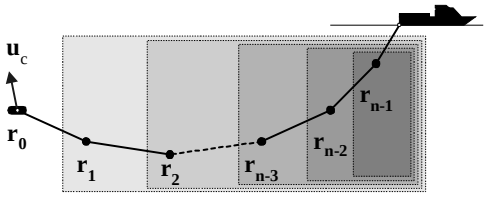

Figure 2: Backstepping along the towed cable.

where $W_1(\eta)$ is positive definite. Using the change of variables

$$\begin{aligned} \mathbf{z} &= \boldsymbol{\xi} - \phi_1 \\ \mathbf{v} &= \mathbf{u}_a - (\partial\phi_1/\partial\boldsymbol{\eta})\,\dot{\boldsymbol{\eta}} \end{aligned} \tag{31}$$

(28)–(29) can be rewritten as

$$\dot{\boldsymbol{\eta}} = \mathbf{f} + \mathbf{G}\phi_1 + \mathbf{G}\mathbf{z} \tag{32}$$

$$\dot{\mathbf{z}} = \mathbf{v} \tag{33}$$

which is similar to the system we started from in (28)–(29), except that now the first component, $\mathbf{f} + \mathbf{G}\phi_1$, has an asymptotically stable origin when the input is zero. This feature will be exploited in the design of $\mathbf{v}$ via $\mathbf{e}_3$ to stabilize the system. Consider the Lyapunov function

$$V_2(\boldsymbol{\eta}, \mathbf{z}) = V_1(\boldsymbol{\eta}) + V_z(\mathbf{z}) = \frac{1}{2}\boldsymbol{\eta}^T\boldsymbol{\eta} + \frac{1}{2}\mathbf{z}^T\mathbf{z} \tag{34}$$

where $V_1(\boldsymbol{\eta})$ satisfies the inequality (30). Taking the time derivative of $V_2(\boldsymbol{\eta}, \mathbf{z})$ along the trajectories of (32)–(33) gives

$$\begin{aligned} \dot{V}_2 &= \frac{\partial V_1}{\partial \boldsymbol{\eta}}\dot{\boldsymbol{\eta}} + \frac{\partial V_z}{\partial \mathbf{z}}\dot{\mathbf{z}} \\ &= \frac{\partial V_1}{\partial \boldsymbol{\eta}}\left[\mathbf{f} + \mathbf{G}\phi_1 + \mathbf{G}\mathbf{z}\right] + \mathbf{z}^T\mathbf{v} \\ &= \frac{\partial V_1}{\partial \boldsymbol{\eta}}\left[\mathbf{f} + \mathbf{G}\phi_1\right] + \left[\mathbf{G}\left(\frac{\partial V_1}{\partial \boldsymbol{\eta}}\right)^T + \mathbf{v}\right]^T \mathbf{z} \end{aligned} \tag{35}$$

and choosing $\mathbf{u}_a$ in (31) as

$$\mathbf{u}_a = \frac{\partial \phi_1}{\partial \boldsymbol{\eta}}\dot{\boldsymbol{\eta}} - \mathbf{G}\left(\frac{\partial V_1}{\partial \boldsymbol{\eta}}\right)^T - k_1\mathbf{z} \tag{36}$$

where $k_1 > 0$, gives

$$\dot{V}_2 \leq -W_1(\boldsymbol{\eta}) - k_1\mathbf{z}^T\mathbf{z} \tag{37}$$

which shows that the origin of (32)–(33) is asymptotically stable. Restoring the input transformation in (27) and the change of variables that were introduced earlier in the derivations, gives the control law for $\mathbf{e}_3$

$$\begin{aligned} \mathbf{u} = \phi_2 &= \mathbf{G}_a^{-1}\left[\frac{\partial \phi_1}{\partial \boldsymbol{\eta}}\dot{\boldsymbol{\eta}} - \mathbf{G}\left(\frac{\partial V_1}{\partial \boldsymbol{\eta}}\right)^T - k_1\left[\boldsymbol{\xi} - \phi_1\right] - \mathbf{f}_a\right] \\ &= \mathbf{G}_2^{-1}\left[\frac{\partial \phi_1}{\partial \mathbf{e}_1}\left[\mathbf{f}_1 + \mathbf{G}_1\mathbf{e}_2\right]\right. \\ &\quad \left. - \mathbf{G}_1\left(\frac{\partial V_1}{\partial \mathbf{e}_1}\right)^T - k_1\left[\mathbf{e}_2 - \phi_1\right] - \mathbf{f}_2\right] \end{aligned} \tag{38}$$

3.1.2 Design of e_4 as Control Input

Next, we consider the system in (21)–(23) as a special case of (21)–(22) with

$$\begin{aligned} \boldsymbol{\eta} &= \begin{pmatrix} \mathbf{e}_1 \\ \mathbf{e}_2 \end{pmatrix}, \qquad \boldsymbol{\xi} = \mathbf{e}_3 \\ \mathbf{f}(\boldsymbol{\eta}) &= \begin{pmatrix} \mathbf{f}_1 + \mathbf{G}_1 e_2 \\ \mathbf{f}_2 \end{pmatrix}, \qquad \mathbf{G}(\boldsymbol{\eta}) = \begin{pmatrix} 0 \\ \mathbf{G}_2 \end{pmatrix} \\ \mathbf{f}_a(\boldsymbol{\eta}, \xi) &= \mathbf{f}_3(\mathbf{e}_1, \ldots, \mathbf{e}_3) \\ \mathbf{G}_a(\boldsymbol{\eta}, \xi) &= \mathbf{G}_3(\mathbf{e}_1, \ldots, \mathbf{e}_3) \\ \mathbf{u} &= \mathbf{e}_4 \end{aligned}$$

This gives

$$\dot{\boldsymbol{\eta}} = \mathbf{f}(\boldsymbol{\eta}) + \mathbf{G}(\boldsymbol{\eta})\boldsymbol{\xi} \tag{39}$$

$$\dot{\boldsymbol{\xi}} = \mathbf{f}_a(\boldsymbol{\eta}, \boldsymbol{\xi}) + \mathbf{G}_a(\boldsymbol{\eta}, \boldsymbol{\xi})\,\mathbf{u} \tag{40}$$

Assume that $\mathbf{G}_a(\eta, \boldsymbol{\xi}) \neq \mathbf{0}$. Using the input transformation

$$\mathbf{u}_a = \mathbf{f}_a(\boldsymbol{\eta}, \boldsymbol{\xi}) + \mathbf{G}_a(\boldsymbol{\eta}, \boldsymbol{\xi})\,\mathbf{u} \tag{41}$$

in (39)–(40) gives

$$\dot{\boldsymbol{\eta}} = \mathbf{f}(\boldsymbol{\eta}) + \mathbf{G}(\boldsymbol{\eta})\boldsymbol{\xi} \tag{42}$$

$$\dot{\boldsymbol{\xi}} = \mathbf{u}_a \tag{43}$$

Suppose that we can find a smooth state feedback control $\boldsymbol{\xi} = \phi_2(\boldsymbol{\eta})$ such that the origin of $\dot{\boldsymbol{\eta}} = \mathbf{f} + \mathbf{G}\phi_2$ is asymptotically stable. Note that in this case $\phi_2(\boldsymbol{\eta})$ in (38) would be our choice. Suppose further that we know a Lyapunov function $V_2(\eta)$, as given in (34), which satisfies the inequality

$$\frac{\partial V_2(\eta)}{\partial \eta}\left[\mathbf{f} + \mathbf{G}\phi_2\right] \leq -W_2(\eta) \tag{44}$$

where $W_2(\eta)$ is positive definite. Using the change of variables

$$\begin{aligned} \mathbf{z} &= \boldsymbol{\xi} - \phi_2 \\ \mathbf{v} &= \mathbf{u}_a - (\partial\phi_2/\partial\boldsymbol{\eta})\,\dot{\boldsymbol{\eta}} \end{aligned} \tag{45}$$

(42)–(43) can be rewritten as

$$\dot{\boldsymbol{\eta}} = \mathbf{f} + \mathbf{G}\phi_2 + \mathbf{G}\mathbf{z} \tag{46}$$

$$\dot{\mathbf{z}} = \mathbf{v} \tag{47}$$

where the first component, $\mathbf{f} + \mathbf{G}\phi_2$, has an asymptotically stable origin when the input is zero. Now, consider the Lyapunov function

$$V_3 = V_2(\boldsymbol{\eta}) + V_z(\mathbf{z}) = V_2(\boldsymbol{\eta}) + \frac{1}{2}\mathbf{z}^T\mathbf{z} \tag{48}$$

where $V_2(\boldsymbol{\eta})$ satisfies the inequality (44). Taking the time derivative of V_3 along the trajectories of (46)–(47) gives

$$\begin{aligned} \dot{V}_3 &= \frac{\partial V_2}{\partial \boldsymbol{\eta}}\dot{\boldsymbol{\eta}} + \frac{\partial V_z}{\partial \mathbf{z}}\dot{\mathbf{z}} \\ &= \frac{\partial V_2}{\partial \boldsymbol{\eta}}\left[\mathbf{f} + \mathbf{G}\phi_2\right] + \left[\mathbf{G}\left(\frac{\partial V_2}{\partial \boldsymbol{\eta}}\right)^T + \mathbf{v}\right]^T \mathbf{z} \end{aligned} \tag{49}$$

and choosing $\mathbf{u}_a$ in (45) as

$$\mathbf{u}_a = \frac{\partial \phi_2}{\partial \boldsymbol{\eta}}\dot{\boldsymbol{\eta}} - \mathbf{G}\left(\frac{\partial V_2}{\partial \boldsymbol{\eta}}\right)^T - k_2\mathbf{z} \tag{50}$$

where $k_2 > 0$, gives

$$\dot{V}_3 \leq -W_2(\eta) - k_2\mathbf{z}^T\mathbf{z} \tag{51}$$

which shows that the origin of (46)–(47) is asymptotically stable. Restoring the input transformation in (41) and the change of variables that were introduced earlier in the derivations, gives the control law for $\mathbf{e}_4$

$$\begin{aligned} \mathbf{u} = \phi_3 &= \mathbf{G}_3^{-1}\left[\frac{\partial \phi_2}{\partial \mathbf{e}_1}\left[\mathbf{f}_1 + \mathbf{G}_1\mathbf{e}_2\right] + \frac{\partial \phi_2}{\partial \mathbf{e}_2}\left[\mathbf{f}_2 + \mathbf{G}_2\mathbf{e}_3\right]\right. \\ &\quad \left. - \mathbf{G}_2\left(\frac{\partial V_2}{\partial \mathbf{e}_2}\right)^T - k_2\left[\mathbf{e}_3 - \phi_2\right] - \mathbf{f}_3\right] \end{aligned} \tag{52}$$

where ϕ_2 and V_2 are given in (38) and (34), respectively.

3.1.3 Design of $\mathbf{u}_c$ as Control Input

As final step, consider the total system in (21)–(24) as a special case of (21)–(22) with

$$\begin{aligned}
\boldsymbol{\eta} &= \begin{pmatrix} \mathbf{e}_1 \\ \mathbf{e}_2 \\ \mathbf{e}_3 \end{pmatrix}, \qquad \boldsymbol{\xi} = \mathbf{e}_4 \\
\mathbf{f}(\boldsymbol{\eta}) &= \begin{pmatrix} \mathbf{f}_1 + \mathbf{G}_1\mathbf{e}_2 \\ \mathbf{f}_2 + \mathbf{G}_2\mathbf{e}_3 \\ \mathbf{f}_3 \end{pmatrix}, \qquad \mathbf{G}(\boldsymbol{\eta}) = \begin{pmatrix} \mathbf{0} \\ \mathbf{0} \\ \mathbf{G}_3 \end{pmatrix} \\
\mathbf{f}_a(\boldsymbol{\eta}, \boldsymbol{\xi}) &= \mathbf{f}_4(\mathbf{e}_1, \ldots, \mathbf{e}_4) \\
\mathbf{G}_a(\boldsymbol{\eta}, \boldsymbol{\xi}) &= \mathbf{G}_4(\mathbf{e}_1, \ldots, \mathbf{e}_4) \\
\mathbf{u} &= \mathbf{u}_c
\end{aligned}$$

Similar to the previous derivations, with the state feedback control $\boldsymbol{\xi} = \phi_3(\boldsymbol{\eta})$ and the change of variable $\mathbf{z} = \boldsymbol{\xi} - \phi_3$, together with the Lyapunov function

$$V_4 = V_3(\boldsymbol{\eta}) + V_z(\mathbf{z}) = V_3(\boldsymbol{\eta}) + \frac{1}{2}\mathbf{z}^T\mathbf{z} \tag{53}$$

we can obtain

$$\mathbf{u}_c = \mathbf{G}_a^{-1}\left[\frac{\partial \phi_3}{\partial \boldsymbol{\eta}}\dot{\boldsymbol{\eta}} - \mathbf{G}\left(\frac{\partial V_3}{\partial \boldsymbol{\eta}}\right)^T - k_3\mathbf{z} - \mathbf{f}_a\right]$$

where $k_3 > 0$. The boundary control law $\mathbf{u}_c$, which is constructed using (34), (38), (48), (52) and

$$\phi_1 = -x_{2d} - k_0\mathbf{e}_1, \quad k_0 > 0$$

recursively, will thus asymptotically stabilize the origin of (21)–(24). We can now express the boundary control law as

$$\begin{aligned}
\mathbf{u}_c &= \mathbf{G}_4^{-1}\left[\frac{\partial \phi_3}{\partial \mathbf{e}_1}[\mathbf{f}_1 + \mathbf{G}_1\mathbf{e}_2] + \frac{\partial \phi_3}{\partial \mathbf{e}_2}[\mathbf{f}_2 + \mathbf{G}_2\mathbf{e}_3]\right. \\
&\quad + \frac{\partial \phi_3}{\partial \mathbf{e}_3}[\mathbf{f}_3 + \mathbf{G}_3\mathbf{e}_4] \\
&\quad \left. - \mathbf{G}_3\left(\frac{\partial V_3}{\partial \mathbf{e}_3}\right)^T - k_3[\mathbf{e}_4 - \phi_3] - \mathbf{f}_4\right]
\end{aligned} \tag{54}$$

The boundary control law $\mathbf{u}_c$ can be designed recursively through the states $\mathbf{e}_j$ for $j = 2, ..., 2n$. A general expression can be written as

$$\mathbf{u}_c = \phi_j = \mathbf{G}_j^{-1}\{A_j + B_j + C_j\} \tag{55}$$

where

$$\begin{aligned}
A_j &= \sum_{i=2}^{j}\left[\frac{\partial \phi_{j-1}(\mathbf{e}_1, ..., \mathbf{e}_{i-1})}{\partial \mathbf{e}_{i-1}}\dot{\mathbf{e}}_{i-1}\right] \\
B_j &= -\mathbf{G}_{j-1}\left[\frac{\partial V_{j-1}(\mathbf{e}_1, ..., \mathbf{e}_{i-1})}{\partial \mathbf{e}_{j-1}}\right]^T \\
C_j &= -k_{j-1}\left[\mathbf{e}_j - \phi_{j-1}\right] - \mathbf{f}_j
\end{aligned}$$

4 Simulation and Numerical Results

The boundary control (54) together with the system (21)–(24) is solved numerically. The results of the simulation are shown in Figure 3-4. In the simulations, a towed cable of length $150\,\mathrm{m}$ is discretized with $n = 2$. The parameters used in the simulation are

$\boldsymbol{v}$	$= (-2, 0, 0)^T\ \mathrm{m/s}$	m_a	$= 8\,\mathrm{kg}$
$\mathbf{r}_2$	$= (200, 0, 0)^T\ \mathrm{m}$	V_a	$= 0.0078\,\mathrm{m}^3$
$\mathbf{g}$	$= (0, 0, 9.81)^T\ \mathrm{m/s}^2$	E	$= 3 \times 10^9\ \mathrm{N/m}^2$
d	$= 0.08\,\mathrm{m}$	μ	$= 10^{-4}$
l	$= 75\,\mathrm{m}$	C_{dt}	$= 0.03$
ρ_w	$= 1025\,\mathrm{kg/m}^3$	C_{nt}	$= 0.08$
ρ_c	$= 1127.5\,\mathrm{kg/m}^3$	$d_{1,..,3}$	$= 0.1$
$k_{1,2}$	$= 1$	$k_{3,4}$	$= 5$

The boundary controller is assigned to control the motion of the inner node $\mathbf{r}_1$ via the outer node $\mathbf{r}_0$, and suppress the vibrations along the cable which are assumed to have been caused by the temporary external disturbances through the node $\mathbf{r}_1$. The initial disturbed cable configuration and the desired configuration are calculated in advance by setting the time derivated terms to zero in (21)–(24). Those are calculated to be

Initial configuration	Desired configuration
$\mathbf{x}_1 = (0, 0, -80)^T$	$\mathbf{x}_{1d} = (0, 0, -80)^T$
$\mathbf{x}_2 = (0, 0, 0)^T$	$\mathbf{x}_{2d} = (0, 0, 0)^T$
$\mathbf{x}_3 = (100, 0, -44)^T$	$\mathbf{x}_{3d} = (99.844, 0, -40.144)^T$
$\mathbf{x}_4 = (0, 0, 0)^T$	$\mathbf{x}_{4d} = (0, 0, 0)^T$

Figure 3 shows the position trajectory of motion of the node $\mathbf{r}_1$, which corresponds to the error state $\mathbf{e}_1$, in the controlled and uncontrolled mode. In the uncontrolled mode, $\mathbf{e}_{1,uncontrolled}$, as one could expect, the node $\mathbf{r}_1$ moves to a new position due to the disturbance, and in the absence of the disturbance the node $\mathbf{r}_1$ is forced back to its equilibrium value $\mathbf{r}_{1d}$ by the potential energy stored in the cable structure. However, the hydrodynamic dissipative forces gradually cancel the effect of the stored potential such that the node $\mathbf{r}_1$ converges oscillating to its equilibrium value $\mathbf{r}_{1d}$. In the controlled mode, $\mathbf{e}_{1,controlled}$, the boundary control $\mathbf{u}_c$ actively drives the node $\mathbf{r}_1$ to its equilibrium value $\mathbf{r}_{1d}$, increasing the convergence rate of the node, and suppressing the vibration caused by the disturbance. The boundary controller $\mathbf{u}_c$ thus improves the transient dynamics and enables smooth tracking of the towed cable system. Figure 4 shows the magnitudes of the position error states $\mathbf{e}_1$ and $\mathbf{e}_3$ in the controlled mode. As seen in the figure, $\mathbf{e}_3$ being at rest at the start, converges back to its desired value $\mathbf{e}_{3d}$ as $\mathbf{e}_1$ converges to zero, thus reaching its desired value $\mathbf{e}_{1d}$. It should be noted that the controller complexity increases recursively as the order of aproximations increases, as can be seen from (55). This can be considered a drawback, which is generally the case in backsteppping designs. The results from the simulations validates the proposed control law as expected from theory.

5 Conclusions

A boundary control design for towed cables via backstepping has been presented. A towed cable model is discretized by

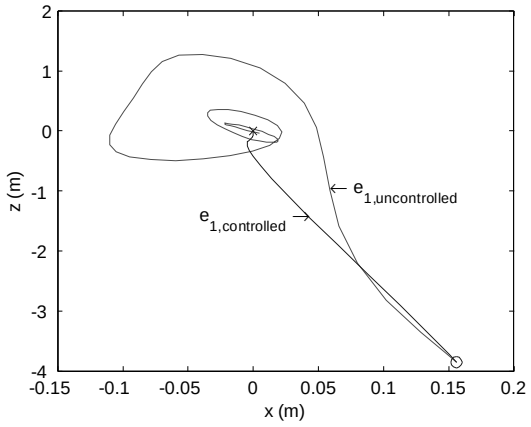

Figure 3: The position trajectory of motion of the inner node $\mathbf{r}_1$, which corresponds to the error state $\mathbf{e}_1$, in the controlled and uncontrolled mode. $\circ$ is the start point and $\times$ is the end point of the motion trajectories in both modes.

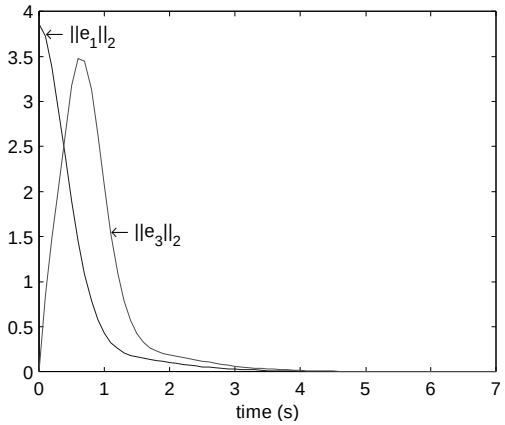

Figure 4: Magnitude of the position errors at the nodes $\mathbf{r}_0$ and $\mathbf{r}_1$ in the controlled mode.

the finite element method into n nodes. The boundary control law has been designed using the states at the outer nodes as inputs to stabilize the states at the inner nodes, thus moving backwards to construct a controller that can stabilize all system states asymptotically. The boundary controller has shown to improve the transient dynamics, suppress the vibrations and enables smooth tracking for the towed cable system. Simulation and numerical results have been presented to validate the proposed boundary control law.

6 Acknowledgement

This work was funded by the Norwegian Research Council under the Strategic University Program in Marine Cybernetics.

References

[1] O. M. Aamo and T. I. Fossen. Finite element modelling of mooring lines. *Mathematics and Computers in Simulations*, 53:415–422, 2000.

[2] C. F. Baicu, C. D. Rahn, and D. M. Dawson. Exponentially stabilizing boundary control of string-mass systems. *J. Vib. and Cont.*, 5:491–502, 1999.

[3] H. Canbolat, D. Dawson, and S. P. Nagarkatti. Boundary control for a general class of string models. Pennsylvania, June 1998. American Control Conf.

[4] Y. Choo and M. J. Casarella. A survey of analytical methods for dynamic simulation of cable-body systems. *J. Hydronautics*, 7:137–144, 1973.

[5] A. P. Dowling. The dynamics of towed cylinders. part 1. neutrally buoyant elements. *J. Fluid Mechanics*, 187:507–532, 1988.

[6] H. P. Lin and N. C. Perkins. Free vibration of complex cable / mass systems: Theory and experiment. *J. Sound and Vib.*, 179:131–149, 1993.

[7] Ö. Morgül. A dynamic control law for the wave equation. *Automatica*, 30:1785–1792, 1994.

[8] M. P. Päidoussis. Dynamics of cylindrical structures subjected to axial f low. *J. Sound and Vib.*, 29:365–385, 1973.

[9] N. Petit and P. Rouchon. Flatness of heavy chain systems. *J. on Control and Optimization*, 40:475–495, 2001.

[10] Z. Qu. Robust and adaptive boundary control of a strecthed string. Illinois, June 2000. American Control Conf.

[11] S. R. Rao. *The Finite Element Method in Engineering*. Butterworth-Heinemann, 1990.

[12] S. M. Shahruz and C. A. Narasimha. Suppression of vibration in strecthed strings by the boundary control. *J. Sound and Vib.*, 204:835–840, 1997.

[13] M. S. Triantafyllou. *Cable Mechanics with Marine Appl.* Lecture Notes, M.I.T, Cambridge, MA, 1990.